

Complexation Properties of N,N',N'',N''' -[1,4,7,10-Tetraazacyclododecane-1,4,7,10-tetrayltetrakis(1-oxoethane-2,1-diyl)]tetrakis[glycine] (H_4 dotagl). Equilibrium, Kinetic, and Relaxation Behavior of the Lanthanide(III) Complexes

by Zsolt Baranyai, Ernő Brücher*, Tímea Iványi, Róbert Király, István Lázár, and László Zékány

Department of Inorganic and Analytical Chemistry, University of Debrecen, P.O. Box 21, H-4010 Debrecen
(fax: +36-52-489-667; e-mail: ebrucher@delfin.klte.hu)

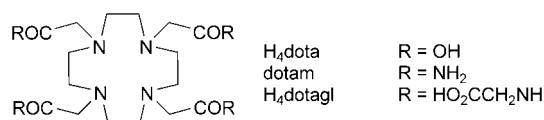
Dedicated to Professor *André E. Merbach* on the occasion of his 65th birthday

Eu^{3+} , Dy^{3+} , and Yb^{3+} complexes of the dota-derived tetramide N,N',N'',N''' -[1,4,7,10-tetraazacyclododecane-1,4,7,10-tetrayltetrakis(1-oxoethane-2,1-diyl)]tetrakis[glycine] (H_4 dotagl) are potential CEST contrast agents in MRI. In the $[Ln(\text{dotagl})]$ complexes, the Ln^{3+} ion is in the cage formed by the four ring N-atoms and the amide O-atom donor atoms, and a H_2O molecule occupies the ninth coordination site. The stability constants of the $[Ln(\text{dotagl})]$ complexes are *ca.* 10 orders of magnitude lower than those of the $[Ln(\text{dota})]$ analogues ($H_4\text{dota} = 1,4,7,10$ -tetraazacyclododecane-1,4,7,10-tetraacetic acid). The free carboxylate groups in $[Ln(\text{dotagl})]$ are protonated in the pH range 1–5, resulting in mono-, di-, tri-, and tetraprotonated species. Complexes with divalent metals (Mg^{2+} , Ca^{2+} , and Cu^{2+}) are also of relatively low stability. At $pH > 8$, Cu^{2+} forms a hydroxo complex; however, the amide H-atom(s) does not dissociate due to the absence of anchor N-atom(s), which is the result of the rigid structure of the ring. The relaxivities of $[Gd(\text{dotagl})]$ decrease from 10 to 25°, then increase between 30–50°. This unusual trend is interpreted with the low H_2O -exchange rate. The $[Ln(\text{dotagl})]$ complexes form slowly, *via* the equilibrium formation of a monoprotonated intermediate, which deprotonates and rearranges to the product in a slow, OH^- -catalyzed reaction. The formation rates are lower than those for the corresponding $Ln(\text{dota})$ complexes. The dissociation rate of $[Eu(\text{dotagl})]$ is directly proportional to $[H^+]$ (0.1–1.0M $HClO_4$); the proton-assisted dissociation rate is lower for $[Eu(H_4\text{dotagl})]$ ($k_1 = 8.1 \cdot 10^{-6} \text{ M}^{-1} \text{ s}^{-1}$) than for $[Eu(\text{dota})]$ ($k_1 = 1.4 \cdot 10^{-5} \text{ M}^{-1} \text{ s}^{-1}$).

Introduction. – Paramagnetic gadolinium(III) complexes of several polyazapoly-carboxylate ligands are widely applied as contrast-enhancement agents in magnetic resonance imaging (MRI) [1][2]. The chelating ligands used are the open-chain dtpa, the macrocyclic dota or their derivatives ($H_3\text{dtpa} = \text{diethylenetriamine-}N,N,N',N''$ -pentaacetic acid = N,N -bis[2-[bis(carboxymethyl)amino]ethyl]glycine; $H_4\text{dota} = 1,4,7,10$ -tetraazacyclododecane-1,4,7,10-tetraacetic acid). These ligands are all octadentate, and the ninth coordination site of Gd^{3+} is occupied by a H_2O molecule. The presence of this H_2O molecule in the inner sphere is highly important in transferring the paramagnetic effect of Gd^{3+} to the bulk water, which will result in an increase of the longitudinal relaxation rate of water protons in body fluids and tissues. The rate of H_2O exchange between the inner sphere and the bulk is a significant parameter in determining the relaxation effect of the Gd^{3+} complex. ^{17}O -NMR Data indicated that the rate of H_2O exchange of the clinically used complexes like $[Gd(\text{dtpa})]$ and $[Gd(\text{dota})]$ was considerably lower than the optimal values (the charge of complexes will be given only when it is absolutely necessary) [1–3]. In lanthanide(III) (Ln^{3+})

complexes of dota tetramide derivatives, even lower H₂O exchange rates have been measured [4–6]. Such Ln³⁺ complexes containing a slowly exchanging H₂O molecule and amide protons have been proposed as paramagnetic chemical exchange saturation transfer (CEST) contrast agents in MRI [7–11]. In the CEST technique, first described by *Balaban* and co-workers [12], a frequency-selective RF pulse is applied at the resonance frequency of the exchangeable OH and/or NH protons of some metabolites, which exchange with the protons of bulk water, reducing the signal intensity of the water due to a saturation-transfer effect [12]. Since the OH and NH proton signals are shifted less than *ca.* 5 ppm from the bulk-water signal, it is difficult to avoid the off-resonance direct saturation of the bulk-water signal.

It is known that certain paramagnetic Ln³⁺ ions (*e.g.*, Eu³⁺, Dy³⁺, Yb³⁺) result in large hyperfine shifts of the surrounding protons. Consequently, the signals of the exchangeable amide and inner-sphere H₂O protons of the dota tetramide derivative complexes are strongly shifted from the bulk-water signal. Such strongly shifted signals can be successfully used in CEST experiments. For the complexation of Ln³⁺ ions, *Aime* and co-workers suggested the ligand ‘1,4,7,10-tetraazacyclododecane-1,4,7,10-tetraacetyl-glycine’ (= *N,N',N'',N'''*-[1,4,7,10-tetraazacyclododecane-1,4,7,10-tetra-yltetrakis-(1-oxoethane-2,1-diyl)]tetrakis[glycine]; H₄dotagl) [9][10]. Ln³⁺ Complexes formed with the tetraethyl ester derivative of H₄dotagl have also been proposed by *Sherry* and co-workers as CEST agents [7][8]. In the Ln(dotagl) complexes, the Ln³⁺ ion is in the coordination cage formed by the four ring N-atoms and four amide O-atoms, while the glycine carboxylate groups are not coordinated. In the inner sphere of the Ln³⁺, a H₂O molecule occupies the ninth coordination site [7][9][10].



The formation and more particularly the dissociation rate of the [Ln(dotagl)] complexes has been expected to be very low, similarly to [Ln(dota)] chelates, though neither the equilibrium nor the kinetic properties were studied in detail. The objective of the present study was to investigate the solution equilibria as well as the formation and dissociation kinetics of dotagl complexes formed with a series of Ln³⁺ ions. Additionally, relaxation properties of [Gd(dotagl)] are also reported. The results obtained here for [Ln(dotagl)] complexes are compared to the [Ln(dota)] analogues.

Results and Discussion. – *Equilibrium Studies.* The H₄dotagl ligand can be regarded as a cyclen derivative possessing four acetyl-glycine functional groups attached to the ring N-atoms. On complex formation, the four ring N-atoms and amide O-atoms (or amide N-atoms if the amide H-atoms dissociate) will encapsulate the metal ion, hence this coordination cage resembles highly that of the ligand dotam (=1,4,7,10-tetraazacyclododecane-1,4,7,10-tetraacetamide). The acetyl-glycinate functional groups are very weak complexing agents despite the carboxylate and amide O-donor atoms [13].

The protonation constants of dotagl^{4-} ($=\text{L}^{4-}$) and the stability and protonation constants of the metal complexes (K_{ML} ; $K_{\text{MH}_i\text{L}}$) are defined by *Eqns. 1–3*, where $i = 1, 2, 3 \dots$.

$$K_i^{\text{H}} = \frac{[\text{H}_i\text{L}]}{[\text{H}_{i-1}\text{L}][\text{H}^+]} \quad (1)$$

$$K_{\text{MH}_i\text{L}} = \frac{[\text{MH}_i\text{L}]}{[\text{MH}_{i-1}\text{L}][\text{H}^+]} \quad (2)$$

$$K_{\text{ML}} = \frac{[\text{ML}]}{[\text{M}][\text{L}]} \quad (3)$$

The protonation constants of dotagl ($\log K_i^{\text{H}}$) determined by pH potentiometry are listed and compared to those of dota in *Table 1* (standard deviations are shown in parentheses). In general, the presence of amide groups in open-chain or macrocyclic aminopolycarboxylate ligands decreases the basicity of the amine N-atoms [14][15]. The first two protonation constants of dotagl are indeed significantly lower than those of dota . $^1\text{H-NMR}$ spectroscopy evidenced that the first two protons are attached to the ring N-atoms, followed by the protonation of the carboxylate groups [16a].

Table 1. Protonation Constants of the Ligands dotagl (25°, 1.0M KCl) and dota (25°, 0.1M Me_4NCl)

| | dotagl | dota^{a} |
|-----------------------|-----------------|--------------------------|
| $\log K_1^{\text{H}}$ | 9.19(0.02) | 12.6 |
| $\log K_2^{\text{H}}$ | 6.25(0.03) | 9.7 |
| $\log K_3^{\text{H}}$ | 4.08(0.04) | 4.5 |
| $\log K_4^{\text{H}}$ | 3.45(0.04) | 4.14 |
| $\log K_5^{\text{H}}$ | 3.20(0.03) | 2.32 |
| $\log K_6^{\text{H}}$ | 1.40(0.05) | – |

^a) From [28].

The $^1\text{H-NMR}$ titration of dotagl with NaOD in $\text{D}_2\text{O}/\text{H}_2\text{O}$ shows significant changes in the chemical shifts of the nonlabile protons (*Fig. 1*). The spectra are rich in signals, particularly between pH 5 and 9. In this pH range, the partially protonated free ligand and the Na^+ complex are present, and the ligand exchange between $[\text{NaL}]$ and L is presumably slow. Above pH 9, the $[\text{NaL}]$ complex predominates. In the pH range 5–9, the signals of the acetyl and ring methylene protons are shifted, indicating the protonation of the ring N-atoms. The glycinate methylene signals are affected only at $\text{pH} < 5$ resulting from the protonation of the carboxylate groups. It has to be noted that with the exception of the glycinate methylene groups, all protons gave broad and split signals at $\text{pH} < 5$, which made the chemical-shift determination fairly difficult. Moreover, the splitting of the signals corresponding to the ring methylene and neighboring acetyl methylene groups indicates that rigid conformers form on protonation. The $\log K_5^{\text{H}}$ value of dotagl , which characterizes the protonation of the

third carboxylate, is significantly higher than that of dota. This originates from the large distance between the carboxylate groups and the protonated ring N-atoms.

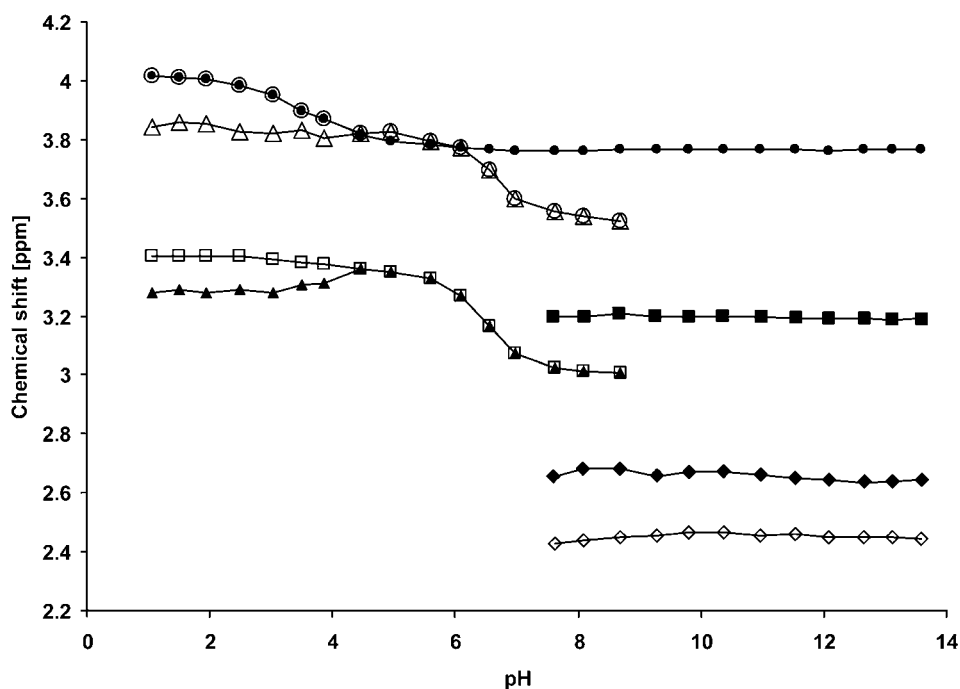


Fig. 1. Chemical shifts of the nonlabile protons of dotagl (L). Legends: ring CH₂, □ and ▲ for L, ◆ and ◇ for the sodium complex of L; acetyl CH₂, ○ and △ for L, ■ for the sodium complex of L; glycine CH₂, ● in both species of L.

The lower basicity of the ring N-atoms in dotagl results in a significantly lower stability for the complexes as compared to the dota analogues. The stability constants obtained by direct pH-potentiometric titration for the divalent metals (M²⁺) and by the ‘out-of-cell’ technique for the lanthanides are presented in *Table 2*.

In the [Ln(dotagl)] complexes, the Ln³⁺ ions are coordinated by the four ring N-atoms and four amide O-atoms as evidenced by solution NMR, or by X-ray-diffraction studies for the complexes of the dotagl ethyl ester [10][17]. The coordination of only noncharged donor atoms to the Ln³⁺ ions is clearly responsible for the low stability of the complexes. The four glycine carboxylates of the ligand are not coordinated and consequently can be protonated to form [Ln(H_idotagl)] species. Interestingly, by titrating the complexes with acid, four protonation constants can be determined for the lighter lanthanides (before Eu³⁺), while only three for [Dy(dotagl)]⁻, and two for [Yb(dotagl)]⁻. The protonation of [Ce(dotagl)] results in a significant change of the absorption spectrum. At pH *ca.* 1.5, where practically all free carboxylates are protonated, the spectrum of [Ce(H₄dotagl)]³⁺ is very similar to that of [Ce(dotam)]³⁺. This is not surprising, since in both complexes, only noncharged ring N-atoms and amide O-atoms are coordinated to the Ce³⁺; thus the complex has a 3+ charge

Table 2. Stability Constants ($\log K$) of the Complexes Formed with dotagl and dota, and Protonation Constants of the Complexes $[\text{Ln}(\text{dotagl})]$ (25° , 1.0M KCl)

| | dotagl | | | | | dota [ML] |
|------------------|-------------|------------|---------------------|---------------------|---------------------|--------------------|
| | [ML] | [MHL] | [MH ₂ L] | [MH ₃ L] | [MH ₄ L] | |
| Mg ²⁺ | 4.34(0.03) | – | – | – | – | 11.92 ^a |
| Ca ²⁺ | 10.39(0.01) | 4.23(0.02) | 3.98(0.04) | 3.96(0.02) | 3.00(0.03) | 17.23 ^a |
| Cu ²⁺ | 13.39(0.06) | 4.38(0.07) | 3.35(0.07) | 3.46(0.07) | – | 22.25 ^a |
| La ³⁺ | 11.84(0.03) | 3.36(0.02) | 3.14(0.02) | 2.41(0.02) | 1.8(0.02) | 22.9 ^b |
| Ce ³⁺ | 13.02(0.05) | 3.38(0.02) | 3.09(0.01) | 2.38(0.02) | 1.9(0.01) | 23.4 ^b |
| Nd ³⁺ | 14.55(0.09) | 3.27(0.02) | 3.02(0.02) | 2.29(0.02) | 1.7(0.02) | 23.0 ^b |
| Eu ³⁺ | 14.84(0.08) | 3.45(0.01) | 2.96(0.01) | 2.40(0.01) | 1.9(0.01) | 23.5 ^b |
| Gd ³⁺ | 14.54(0.09) | 3.38(0.01) | 2.87(0.01) | 2.40(0.01) | – | 24.7 ^b |
| Dy ³⁺ | 14.37(0.05) | 3.30(0.05) | 3.11(0.03) | 1.6(0.06) | – | 24.8 ^b |
| Yb ³⁺ | 14.25(0.02) | 3.07(0.05) | 3.05(0.02) | – | – | 25.0 ^b |

^a) [16b]. ^b) [1] (p. 254).

(Fig. 2). These experiments as well as the low stability constants of dotam complexes [18] indicate that the carboxylate groups may play some role in the complex formation by changing the environment around the coordination cage.

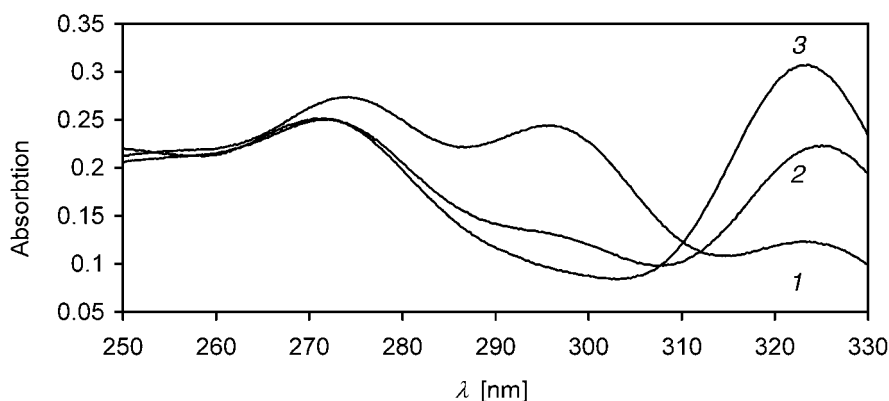


Fig. 2. Absorption spectra of $[\text{Ce}(\text{dotagl})]^-$ (pH 7.96; 1), $[\text{Ce}(\text{H}_4\text{dotagl})]^{3+}$ (pH 1.53; 2), and $[\text{Ce}(\text{dotam})]^{3+}$ (pH 6.56; 3). The concentrations of Ce^{3+} and the ligands were $5 \cdot 10^{-4}$ M.

The stability constants of $[\text{Ln}(\text{dotagl})]$ complexes increase from La^{3+} to Nd^{3+} , then they remain practically constant for the heavier lanthanides with a slight decrease in the end of the series. A similar trend has been observed for $[\text{Ln}(\text{dotam})]^{3+}$ complexes [18]. It clearly indicates that the size match between the lanthanide ion and the coordination cage determined by the ring N-atoms and amide O-atoms is the best for Nd^{3+} – Eu^{3+} .

The dotagl complexes of divalent metal ions also have significantly lower stability as compared to the dota complexes. $[\text{Mg}(\text{dotagl})]^{2-}$ forms only at $\text{pH} > 5$, and protonated complexes cannot be detected at all (Table 2). Interestingly, the protonation constants of $[\text{Ca}(\text{dotagl})]^{2-}$ and $[\text{Cu}(\text{dotagl})]^{2-}$, which characterize the protonation of the carboxylate groups, are somewhat higher than the $\log K_3^{\text{H}}$, $\log K_4^{\text{H}}$, $\log K_5^{\text{H}}$, and $\log K_6^{\text{H}}$

values of the ligand. Similar phenomena have been reported for dtpa complexes of Cu^{2+} or Zn^{2+} [19]. Moreover, since the carboxylate groups are far from each other, the successive protonation constants of the dotagl complexes do not differ considerably.

For Cu^{2+} complexes of oligopeptides, it is known that the amide H-atom dissociates at pH 4–6 and the amide N-atom (N^-) coordinates to Cu^{2+} if an anchor amine N-atom(s) (e.g., terminal NH_2 group) is present. This structural change results in a significant blue shift in the VIS absorption spectrum (the absorption maximum shifts from ca. 700 nm to ca. 560–620 nm [20]).

In the pH-potentiometric titration of the $[\text{Cu}(\text{dotagl})]^{2-}$ complex, some base was consumed at pH > 8; however, the absorption maxima in the VIS spectra remained at ca. 695 nm. This let us conclude that the amide H-atoms of the acetylglycinate moieties did not dissociate. It seems that a ring N-atoms cannot act as an anchor N-atom, likely due to the rigid structure of the macrocycle. Similarly to $[\text{Cu}(\text{dotagl})]$, a base consumption was also observed in the pH-potentiometric titration of $[\text{Ln}(\text{dotagl})]$ complexes at pH > 8. It has been interpreted by assuming the dissociation of the inner-sphere H_2O molecule according to Eqn. 4, where z is the charge of the metal ion. For the equilibrium constants characterizing Eqn. 4, we obtained values of $\log K_{\text{MLH-1}} = 9.84(0.02)$, $9.61(0.06)$, and $9.18(0.02)$ for La^{3+} , Eu^{3+} , and Cu^{2+} , respectively.



Relaxivity of $[\text{Gd}(\text{dotagl})]$. The effect of the Gd^{3+} complexes on the longitudinal relaxation rate of H_2O protons is generally expressed in terms of their relaxivity. The relaxivity (r_1 in $\text{mm}^{-1} \text{s}^{-1}$) is the increase in the longitudinal relaxation rate induced by 1.0 mM Gd^{3+} concentration. In aqueous solutions of Gd^{3+} complexes, the Gd^{3+} induces relaxation of the protons in the H_2O molecules that diffuse in the proximity of the complex. This effect is defined as the ‘outer sphere’ relaxivity (r_1^{os}). On the other hand, the paramagnetic effect of the Gd^{3+} is transferred to bulk water also *via* the exchange of the inner-sphere H_2O molecule(s), producing the ‘inner sphere’ relaxivity (r_1^{is}). The experimentally obtained relaxivity is the sum of the inner and outer sphere terms ($r_1 = r_1^{\text{is}} + r_1^{\text{os}}$). The relaxivity of Gd^{3+} complexes generally depends on the temperature and the pH of the solution. The relaxivities of $[\text{Gd}(\text{dotagl})]$ obtained at different pH values and temperatures at 9-MHz frequency are shown in Fig. 3.

The r_1 values are relatively low at neutral pH and room temperature ($2.1 \text{ mm}^{-1} \text{ s}^{-1}$), since the H_2O exchange is extremely slow for complexes of Gd^{3+} and dota tetramide derivatives [5][11], hence the inner-sphere contribution becomes negligible. Indeed, the relaxivity of $[\text{Gd}(\text{dotagl})]$ is very similar to that of $[\text{Gd}(\text{ttha})]^{3-}$ and $[\text{Gd}(\text{dotp})]^{5-}$, which do not contain inner-sphere H_2O ; thus their relaxivity is controlled by the r_1^{os} term ($\text{H}_6\text{ttha} = \text{triethylenetetramine-hexaacetic acid} = 3,6,9,12\text{-tetrakis}(\text{carboxymethyl})\text{-}3,6,9,12\text{-tetraazatetradecanedioic acid}$; $\text{H}_8\text{dotp} = [1,4,7,10\text{-cyclododecane-}1,4,7,10\text{-tetrayltetrakis}(\text{methylene})\text{]tetrakis}[\text{phosphonic acid}]$) [14][21]. The relaxivities of $[\text{Gd}(\text{dotagl})]$ are constant in the pH range 5–9. The increase of the relaxivities at pH < 5 is probably the result of the protonation of the carboxylate groups, which leads to fast proton exchange with the bulk water. At pH approximately < 3, the rate of the proton-assisted exchange of the inner-sphere H_2O protons also increases and contributes to the observed relaxivity increase. At pH > 9, the proton-exchange rate between the inner-

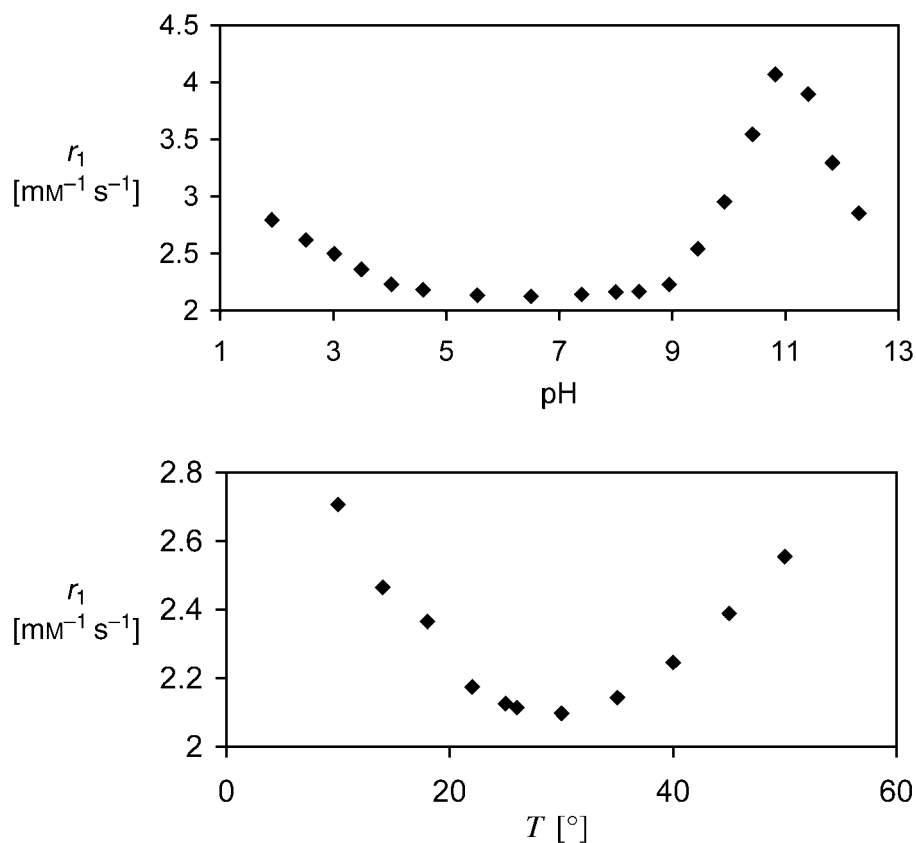


Fig. 3. Relaxivities of $[Gd(dotagl)]$

sphere H_2O and the bulk also increases due to the OH^- -ion catalysis and increases the relaxivity.

The relaxivities of $[Gd(dotagl)]$ show an unusual temperature dependence. For complexes like $[Gd(dtpa)]^{2-}$ or $[Gd(dota)]^-$ with a relatively fast H_2O exchange, both r_1^{is} and r_1^{os} , and consequently r_1 , monotonously decrease with increasing temperature [22]. Contrary to this, for $[Gd(dotagl)]$, the r_1 values decrease in the range $10\text{--}25^{\circ}$, where r_1^{os} predominates, and the diffusion rates of the H_2O molecules and the complex increase with temperature. Further temperature increase above $25\text{--}30^{\circ}$ will accelerate the H_2O exchange, and the increasing contribution from r_1^{is} will exceed the decrease in r_1^{os} , thus the observed relaxivity increases. A relaxivity maximum could likely be observed at a higher temperature, where the H_2O exchange becomes fast enough and a further temperature increase results in lower relaxivities, as observed for $[Gd(dtpa)]^{2-}$. Indeed, a similar trend was reported for the Gd^{3+} complex of the ethyl ester of dotagl [17].

Formation Kinetics of $[Ln(dotagl)]$ Complexes. The first experiences obtained in preparing $[Ln(dotagl)]$ solutions qualitatively indicated that the formation reactions

are very slow. For $[\text{Ln}(\text{dota})]$ complexes, slow complex formation is well-known and has been studied by several groups [23–28]. In the formation of $[\text{Ln}(\text{dota})]$, a diprotonated intermediate forms in a fast reaction, then it slowly deprotonates and transforms to $[\text{Ln}(\text{dota})]$ in an OH^- -catalyzed step [24–28].

The rates of the formation reactions were studied for $[\text{Ce}(\text{dotagl})]$ and $[\text{Eu}(\text{dotagl})]$ by spectrophotometry in the presence of a 10–50 fold Ln^{3+} excess. The formation rates are expressed by Eqn. 5, where k_{obs} is a first-order rate constant (the reactions are of first order even at comparable concentrations of the reactants), and $[\text{L}]_{\text{t}}$ is the total concentration of $\text{H}_x\text{dotagl}^{(4-x)-}$ species. The plot of k_{obs} vs. $[\text{Ln}^{3+}]$ gives a saturation curve which indicates the formation of a reaction intermediate. For $[\text{Ce}(\text{dotagl})]$, this intermediate has been detected by spectrophotometry. As Fig. 4. shows, the aqua complex of Ce^{3+} and the complex $[\text{Ce}(\text{dotagl})]$ have well-distinguished absorption spectra. The presence of the isobestic point, which is shifted from the spectrum of the Ce^{3+} aqua complex, indicates the formation of an intermediate.

$$\frac{d[\text{LnL}]_{\text{t}}}{dt} = k_{\text{obs}}[\text{L}]_{\text{t}} \quad (5)$$

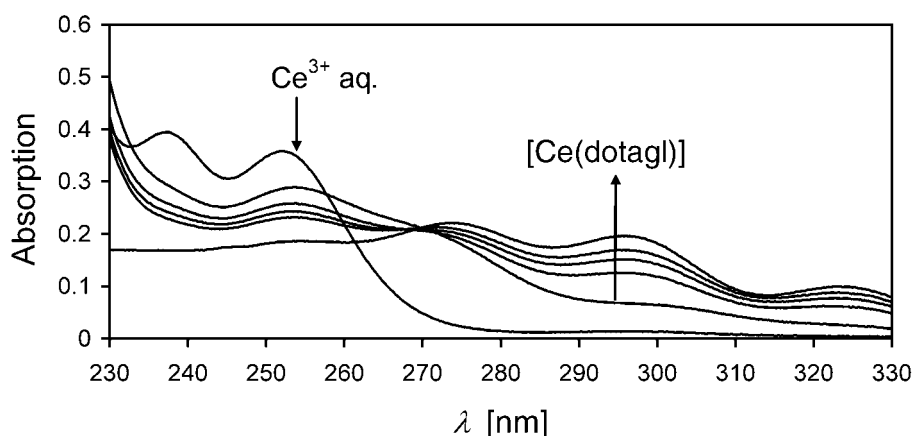


Fig. 4. Absorption spectra of the $[\text{Ce}(\text{dotagl})]$ solution at 0.25 h, 1.25 h, 2.20 h, 3.21 h, and 29.5 h (upwards), after mixing in 0.01M NaOAc. pH 4.85, $[\text{Ce}^{3+}] = [\text{dotagl}] = 5 \cdot 10^{-4}$ M.

Furthermore, on mixing CeCl_3 and $\text{H}_x\text{dotagl}^{(4-x)-}$ in a weakly buffered solution at pH ca. 5, a fast pH drop is observed which is followed by a slow pH decrease, a behavior very similar to that observed in the $[\text{Ce}(\text{dota})]$ system [23][25]. Based on this similarity, we can assume that in the intermediate, the Ln^{3+} is coordinated to the carboxylates and has not yet entered the coordination cage formed by the ring N-atoms and amide O-atoms. Given the significantly lower first two protonation constants of dotagl^{4-} as compared to dota^{4-} , at pH > 4.5 the concentration of the monoprotinated HL^{3-} is not negligible, consequently both mono- and diprotonated intermediates can form (Table 1). In the case of $\text{Ce}(\text{dota})$, we have shown that the mono- and diprotonated

intermediates have identical absorption spectra, indicating that the Ce^{3+} ion has the same coordination environment [28].

The first-order rate constants obtained at different Ln^{3+} concentrations and pH values are presented in Figs. 5 and 6. Figs. 5 and 6 show that the formation rates slightly increase with increasing $[\text{Ln}^{3+}]$, and the k_{obs} values show a second-order dependence on the OH^- concentration.

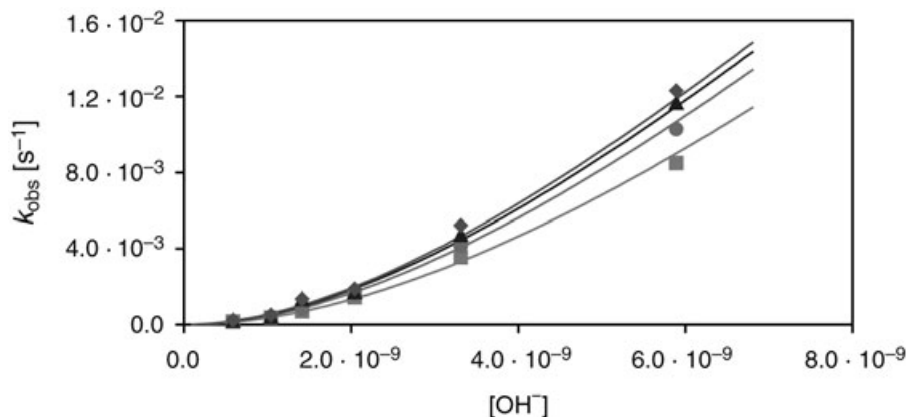


Fig. 5. Formation rates of $[\text{Ce}(\text{dotagl})]$ at 25° , in 1.0M KCl . $[\text{dotagl}] = 3 \cdot 10^{-4}\text{M}$, the concentration of Ce^{3+} was $3 \cdot 10^{-3}\text{M}$ (■), $6 \cdot 10^{-3}\text{M}$ (●), $1 \cdot 10^{-2}\text{M}$ (◆), and $1.5 \cdot 10^{-2}\text{M}$ (▲).

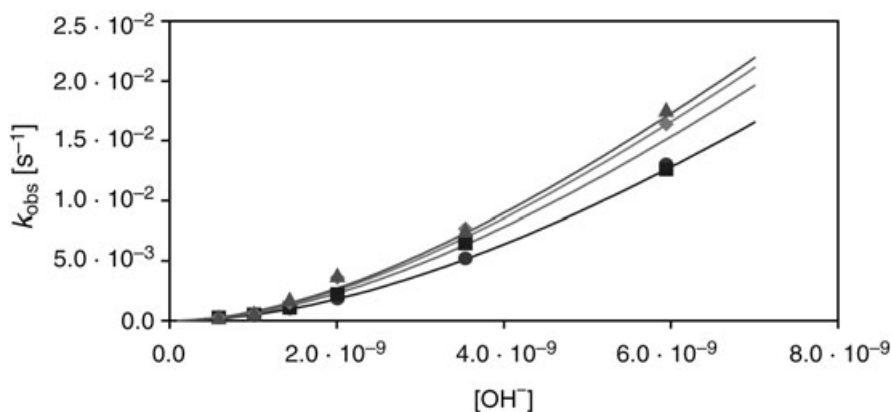
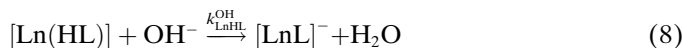
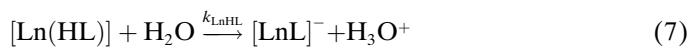
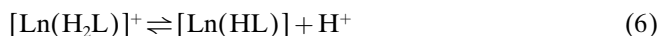


Fig. 6. Formation rates of $[\text{Eu}(\text{dotagl})]$ at 25° , in 1.0M KCl . $[\text{dotagl}] = 3 \cdot 10^{-4}\text{M}$, the concentration of Eu^{3+} was $3 \cdot 10^{-3}\text{M}$ (●), $6 \cdot 10^{-3}\text{M}$ (■), $1 \cdot 10^{-2}\text{M}$ (◆), and $1.5 \cdot 10^{-2}\text{M}$ (▲).

These results can be interpreted by assuming that the rate-determining step in the formation of $[\text{Ln}(\text{dotagl})]$ complexes is the deprotonation and rearrangement of the monoprotonated intermediate, itself in equilibrium with the diprotonated species [25], according to Eqns. 6–8. Eqn. 6 implies an inverse proportionality between $[\text{H}^+]$ and the concentration of the monoprotonated intermediate, thus the formation rate. The deprotonation of the intermediate $[\text{Ln}(\text{HL})]$ is presumably assisted by H_2O molecules

(Eqn. 7). The second-order dependence of k_{obs} on the $[\text{OH}^-]$ can be explained by the OH^- -assisted deprotonation of the intermediate $[\text{Ln}(\text{HL})]$ (Eqn. 8).



By taking into account the total concentration of the Ln^{3+} containing species ($[\text{Ln}^{3+}]_{\text{t}} = [\text{Ln}^{3+}] + [[\text{Ln}(\text{HL})]] + [[\text{Ln}(\text{H}_2\text{L})]]$), the protonation constant of the monoprotonated intermediate $[\text{Ln}(\text{HL})]$, as given by Eqn. 6 ($K_{\text{LnHL}} = [[\text{Ln}(\text{H}_2\text{L})]] / [[\text{Ln}(\text{HL})]][[\text{H}^+]]$), the stability constant of the diprotonated intermediate, K^* ($K^* = [[\text{Ln}(\text{H}_2\text{L})]] / [\text{Ln}^{3+}][[\text{H}_2\text{L}]]$), and Eqn. 5, the first-order rate constant can be expressed by Eqn. 9. We calculated the rate constants and stability constants by fitting the k_{obs} values presented in Figs. 5 and 6 to Eqn. 9. The constants obtained are given and compared to the corresponding values for $[\text{Ce}(\text{dota})]$ in Table 3.

$$k_{\text{obs}} = \frac{k_{\text{LnHL}} + k_{\text{LnHL}}^{\text{OH}} [\text{OH}^-]}{1 + K_{\text{LnHL}}^{\text{H}} [\text{H}^+] + \frac{K_{\text{LnHL}}^{\text{H}} [\text{H}^+]}{K^* [\text{Ln}^{3+}]}} \quad (9)$$

Table 3. Rate Constants Characterizing the Formation of the dotagl and dota Complexes (25°, 1.0M KCl)

| | $[\text{Ce}(\text{dotagl})]^-$ | $[\text{Eu}(\text{dotagl})]^-$ | $[\text{Ce}(\text{dota})]^{-\text{a}}$ |
|---|--------------------------------|--------------------------------|--|
| $k_{\text{LnHL}} [\text{s}^{-1}]$ | – | – | 18.5 |
| $k_{\text{LnHL}}^{\text{OH}} (\text{M}^{-1} \text{s}^{-1})$ | $(4.6 \pm 1) \cdot 10^6$ | $(6.6 \pm 1.6) \cdot 10^6$ | $1.9 \cdot 10^7$ |
| $\log K_{\text{LnHL}}^{\text{H}}$ | 5.8 ± 0.2 | 5.8 ± 0.14 | 8.64 |
| $\log K^*$ | 2.7 ± 0.13 | 2.6 ± 0.14 | 4.5 |

^{a)} [28].

The error in k_{LnHL} is very high, indicating the unimportance of the reaction pathway of Eqn. 7 in the complex formation. The rate constants $k_{\text{LnHL}}^{\text{OH}}$, characterizing the OH^- -assisted formation, are lower for $[\text{Ce}(\text{dotagl})]$ and $[\text{Eu}(\text{dotagl})]$ than for $[\text{Ce}(\text{dota})]$. On the basis of the significantly lower K_1^{H} and K_2^{H} protonation constants of dotagl^{4-} , one could expect higher formation rates for the dotagl complexes. However, in the intermediates $[\text{Ln}(\text{H}_2\text{dotagl})]^+$ and $[\text{Ln}(\text{Hdotagl})]$, Ln^{3+} is coordinated by the carboxylate groups and is, thus, situated further away from the coordination cage than in the corresponding intermediates of dota. This large distance makes it more difficult for the Ln^{3+} to enter into the coordination cage of dotagl and as a result, the complexes form more slowly as compared to the $[\text{Ln}(\text{dota})]$ analogues. The large distance between the carboxylate-coordinated Ln^{3+} ion and the coordination cage is also the reason why the protonation constant of the $[\text{Ln}(\text{Hdotagl})]$ intermediates ($\log K_{\text{LnHL}} = 5.8$) is only slightly lower than that of the monoprotonated ligand itself ($\log K_2^{\text{H}} = 6.25$).

Moreover, the distant position of the carboxylate groups is likely responsible for the low stability constant of the diprotonated intermediates (K^*) as well.

Kinetics of Dissociation of [Eu(dotagl)]. Lanthanide complexes used in medical diagnosis must have high kinetic stability, since the products of dissociation, the free ligand and the Ln^{3+} ion are both toxic. The dissociation of the lanthanide(III) complexes formed with dota and dota derivatives predominantly takes place *via* proton-assisted reactions, and the endogenous metal ions, like Cu^{2+} or Zn^{2+} , have practically no effect on the dissociation rate. The $[\text{Ln}(\text{dotagl})]$ complexes are thermodynamically unstable at $\text{pH} < 1$, thus the dissociation kinetics of $[\text{Eu}(\text{dotagl})]$ was studied in 0.1–1.0M HClO_4 (the sum of the HClO_4 and NaClO_4 concentration was 1.0M). Since the charge-transfer band of Eu^{3+} is sensitive to complex formation, the acid-catalyzed dissociation of $[\text{Eu}(\text{dotagl})]$ was monitored by spectrophotometry at 250 nm where, fortuitous, the complex is the only absorbing species. In the presence of acid excess, the dissociation rate can be given by *Eqn. 10*, where k_p is a pseudo-first-order rate constant. The $k_p (=k_{\text{obs}})$ values determined at different $[\text{H}^+]$ are presented in *Fig. 7*. The dissociation rate is directly proportional to the H^+ concentration according to *Eqn. 11*, where k_0 and k_1 are the rate constants characterizing the spontaneous and proton-assisted dissociation of the complex, respectively. However, it is known from the equilibrium studies (*Table 2*) that at $[\text{H}^+] > 0.1\text{M}$, only the tetraprotonated species, $[\text{Eu}(\text{H}_4\text{dotagl})]^{3+}$ is present practically (each carboxylate group of the ligand is protonated). Therefore, the rate constant k_0 is characteristic for the dissociation of $[\text{Eu}(\text{H}_4\text{dotagl})]^{3+}$, while k_1 characterizes the proton-assisted dissociation of $[\text{Eu}(\text{H}_4\text{dotagl})]^{3+}$. The rate constants calculated from the data as shown in *Fig. 7* are: $k_0 = (7.3 \pm 0.5) \cdot 10^{-7} \text{ s}^{-1}$ and $k_1 = (8.1 \pm 0.2) \cdot 10^{-6} \text{ M}^{-1} \text{ s}^{-1}$. No rate constants have been published for the spontaneous dissociation of $[\text{Eu}(\text{dota})]$; for $[\text{Gd}(\text{dota})]$, Wang *et al.* reported $k_0 < 5 \cdot 10^{-8} \text{ s}^{-1}$ [24].

$$-\frac{d[\text{EuL}]_t}{dt} = k_p[\text{EuL}]_t \quad (10)$$

$$k_p = k_0 + k_1[\text{H}^+] \quad (11)$$

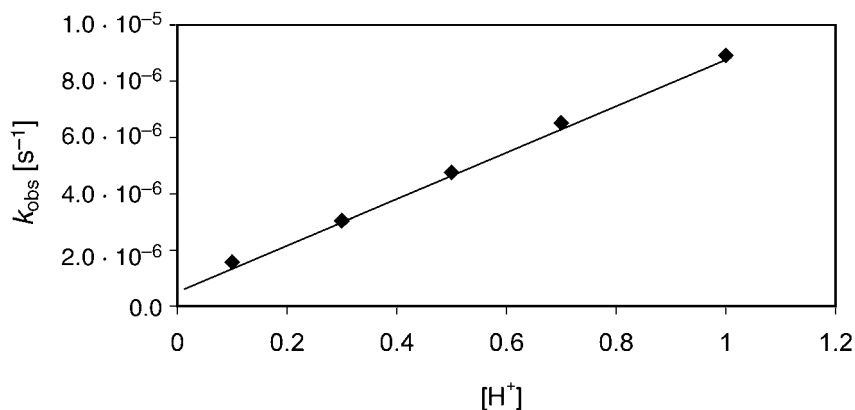


Fig. 7. Rates of dissociation of $[\text{Eu}(\text{dotagl})]$ (25° , $[\text{H}^+] + [\text{NaClO}_4] = 1.0\text{M}$)

For the proton-assisted dissociation of [Eu(dota)], we have previously found $k_1 = 1.4 \cdot 10^{-5} \text{ M}^{-1} \text{ s}^{-1}$ [25]. These data indicate that the proton-assisted dissociation of the tetraprotonated [Eu(H₄dotagl)]³⁺ is slower than that of [Eu(dota)]. On the other hand, the spontaneous dissociation of [Eu(H₄dotagl)]³⁺ seems to be relatively fast in comparison to that of [Eu(dota)]. This is plausible since one of the four carboxylate protons can be easily transferred to a ring N-atom, which results then in dissociation. However, at *ca.* physiological pH, tetraprotonated species do not exist anymore, and the kinetic inertness of [Eu(dotagl)] is high enough for medical applications, as it is predicted from the very low rate of the proton-assisted dissociation of the tetraprotonated complex.

Financial support from the *Hungarian Scientific Research Fund* (OTKA 032100 and OTKA 038364) is gratefully acknowledged. *I. L.* thanks the *Széchenyi István Scholarship* (SZÖ 303/2003) for financial support. This work was carried out within the *European COST-D18* project.

Experimental Part

General. Solvents of reagent grade were purchased from *Spectrum-3D Kft.* (Debrecen, Hungary) and used without further purification, except for MeCN, which was dried with and distilled from CaH₂. Cyclen (= 1,4,7,10-tetraazacyclododecane) and diisopropylethylamine (Pr₂NEt) were obtained from *Aldrich* and distilled from solid KOH pellets and then dry Zn powder. Reagents were purchased from *Aldrich*, *Fluka*, and *Merck* and used without further purification. Column chromatography: silica gel 60 (15–40 μm) from *Merck*. ¹H- and ¹³C-NMR Spectra: *Bruker AM-360* spectrometer; processing with the computer program *MestRe-C 2.3*; solns. in CDCl₃ or D₂O; δ(H) referenced to SiMe₄ or DSS (= 2,2-dimethyl-2-silapentane-5-sulfonic acid) for CDCl₃ or D₂O solns., resp.; δ(C) referenced to CDCl₃ (*t* at δ 77.0) and MeCN (δ 0.3) for CDCl₃ and D₂O solns., resp.

N,N',N'',N'''-[1,4,7,10-Tetraazacyclododecane-1,4,7,10-tetrayltetrakis(1-oxoethane-2,1-diyl)]tetrakis[glycine] Tetrabenzyl Ester (L(Bn)₄). Cyclen (542.9 mg, 3.15 mmol) and Pr₂NEt (4.4 ml, 25 mmol) were dissolved in MeCN (30 ml), and a soln. of *N*-(2-bromoacetyl)glycine benzyl ester (3.61 g, 12.6 mmol) in MeCN (20 ml) was added dropwise over 1 h. The mixture was stirred at r.t. for 4 days, then the solvent was evaporated. The residue was redissolved in CHCl₃ (50 ml), cooled in ice, and extracted with ice-cold 1M NaHCO₃ to remove Pr₂NEt·HBr. The CHCl₃ phase was pre-dried with anh. Na₂SO₄, filtered, further dried with anh. MgSO₄, filtered again, and evaporated. The sticky residue (3.37 g) still contained *ca.* 10–12% of Pr₂NEt·HBr. Therefore, it was dissolved in a small volume of CHCl₃ and subjected to column chromatography (silica gel (100 mg), CHCl₃ (20 ml)) to yield a viscous yellow oil (2.92 g) containing < 6% of Pr₂NEt·HBr (by ¹H-NMR integral ratios): calc. 2.74 g (87%). ¹H-NMR (360 MHz, CDCl₃; SiMe₄): 2.67 (*s*, 16 H, CH₂(ring)); 3.10 (*s*, 8 H, CH₂N); 3.98 (*d*, *J* = 5.79, 8 H, CH₂N); 5.10 (*s*, 8 H, CH₂O); 7.30–7.34 (*m*, 20 arom. H); 7.47 (*t*, *J* = 5.79, 4 H, NH). ¹³C-NMR (90 MHz, CDCl₃): 40.89 (CH₂N); 53.18 (CH₂N); 59.10 (CH₂(ring)); 67.14 (CH₂O); 128.37, 128.49, 128.59 (arom. CH); 135.10 (arom. C); 169.96, 171.55 (C=O).

N,N',N'',N'''-[1,4,7,10-Tetraazacyclododecane-1,4,7,10-tetrayltetrakis(1-oxoethane-2,1-diyl)]tetrakis[glycine] (H₄dotagl, L). H₄dotagl was prepared from the corresponding benzyl ester (L(Bn)₄) by the following procedure, or can be alternatively synthesized by the published method [10]. In a 80-ml pressure-resistant two-necked flask (Hg manometer, N₂-gas inlet line, three-way stopcock for the control of H₂ gas), *N,N',N'',N'''*-[1,4,7,10-tetraazacyclododecane-1,4,7,10-tetrayltetrakis(1-oxoethane-2,1-diyl)]tetrakis[glycine] tetrabenzyl ester (2.73 g; see above) was dissolved in MeOH (50 ml) under dry N₂, and 10% Pd/C (819 mg) was added. The flask was stoppered hermetically and 1 bar of H₂-gas overpressure was applied. When pressure drop ceased (after a few hours at r.t.), the catalyst was filtered off under dry N₂, the filtrate evaporated, and the yellowish oil triturated with MeCN until it solidified. This solid was filtered off on a *Schlenk*-type filter funnel and extracted with hot MeCN to remove Pr₂NEt·HBr yielding a pale yellow solid (1.2 mmol, 44%). ¹H-NMR (360 MHz, pH 4.94 in D₂O/H₂O; DSS): 3.79 (*s*, 2 H, >NCH₂CO); 3.83 (*br. s.*, 1 H, NHCH₂COOH); 3.77 (*br. s.*, 1 H, NHCH₂COOH); 3.35 (*br. s.*, 4 H, CH₂(ring)); 8.27 (CONH). ¹³C-NMR (90 MHz, D₂O; pD 3.0; MeCN as ref. δ 0.3): 42.7 (CH₂(ring)); 55.4 (CH₂N); 175.1 (C=O, overlapping).

Equilibrium Measurements. The chemicals used in the experiments were of the highest anal. grade. For the preparation of the LnCl₃ solns., Ln₂O₃ (*Fluka*; 99.9%) were dissolved in 6.0M HCl, and the excess of acid was

evaporated. The CeCl_3 soln. was prepared from $\text{CeCl}_3 \cdot 7\text{H}_2\text{O}$ (Aldrich; 99.9%). The concentration of the LnCl_3 , MgCl_2 , CaCl_2 , and CuCl_2 solns. were determined by complexometric titration with standardized $\text{Na}_2\text{H}_2\text{edta}$ and xylenol orange (LnCl_3), murexid (CuCl_2), Patton & Reeder (CaCl_2), and eriochrome black T (MgCl_2) as indicator. The concentration of dotagl was determined by pH-potentiometric titration in the presence and absence of a large (40-fold) excess of CaCl_2 .

The protonation constants of dotagl and the stability constants of the complexes formed with Mg^{2+} , Ca^{2+} , and Cu^{2+} were determined by pH-potentiometric titration. The metal-to-ligand concentration ratios were 1:1 but for the Cu^{2+} complexes, titrations were also made at metal-to-ligand ratio 2:1 and 1:2 (the concentration of ligand was generally 2.0 mM). The protonation constants of the complexes $[\text{Ln}(\text{dotagl})]^-$ were determined by pH potentiometry, with the titration of the complexes from pH ca. 6 with HCl. The stability constants of the complexes $[\text{Ln}(\text{dotagl})]^-$ were determined by the 'out-of-cell' technique because of the slow formation reactions. The pH range where complexation equilibria existed and the time needed to reach the equilibria were determined by spectrophotometry for the formation of $[\text{Ce}(\text{dotagl})]$ (the UV absorption band of Ce^{3+} resulting from the 4f-5d transition is very sensitive for complex formation). Eight Ln^{3+} (2 mM)/dotagl (2 mM) samples (4 ml) were prepared in duplicate which in equilibrium had pH values in the range 2.6–3.8. The samples were 1.0M in KCl to maintain constant ionic strength. The closed samples were kept at 25° for 5 weeks to reach the equilibria. For the calculation of the stability constants of complexes $[\text{Ln}(\text{dotagl})]^-$ beside the protonation constants of the ligand, the protonation constants of the complexes were also used, which were determined in separate titration experiments.

For the calculation of $[\text{H}^+]$ from the measured pH values, the method proposed by Irving *et al.* was used [29]. A 0.01M HCl soln. (1.0M for KCl) was titrated with the standardized KOH soln. The differences between the measured and calculated pH values were used to obtain the H^+ concentrations from the pH values, measured in the titration experiments.

For the pH measurements and titrations, a Radiometer PHM93 pH meter, an ABU 80 autoburette, and a Metrohm 6.0234.100 combined electrode were used. The titrated sample (5 ml) was thermostated at 25°. The solns. were stirred, and N_2 was bubbled through them. The titrations were made in the pH range 1.7–11.7. For the calibration of the pH meter, KH-phthalate (pH 4.005) and borax (pH 9.180) buffers were used.

The protonation and stability constants were calculated with the program PSEQUAD [30].

Measurement of Relaxation Times. The relaxivity values were calculated from the longitudinal relaxation times of H_2O protons (T_1) measured with an MS-4 NMR spectrometer (Institute Jozef Stefan, Ljubljana) at 9 MHz. The temp. of the sample holder was controlled with a thermostated air stream. The longitudinal relaxation times were measured by the 'inversion recovery' method ($180^\circ - \tau - 90^\circ$) by using 6–8 different τ values. The measurements were made with 1.0 mM $[\text{Gd}(\text{dotagl})]$ solns., so the relaxivity was given as $r_1 = 1/T_{1m} - 1/T_{1w}$, where T_{1m} and T_{1w} are the relaxation times measured in the presence and absence of the $[\text{Gd}(\text{dotagl})]$.

Kinetic Studies. The rates of the formation reactions were studied by spectrophotometry at 25° in a thermostated cell holder with a Cary 1E spectrophotometer. The formation rates of $[\text{Ce}(\text{dotagl})]$ and $[\text{Eu}(\text{dotagl})]$ were followed at 320 and 250 nm, resp., in 1.0M KCl. The concentration of the ligand dotagl was $3 \cdot 10^{-4}$ M, while the concentration of the Ce^{3+} and Eu^{3+} was 10 to 50 times higher. For keeping the pH values constant, an *N*-methylpiperazine buffer (0.03M) was used.

The rates of dissociation of the complex $[\text{Eu}(\text{dotagl})]$ in 0.1–1.0M HClO_4 ($[\text{HClO}_4] + [\text{NaClO}_4] = 1.0\text{M}$) were monitored by spectrophotometry at 250 nm. The concentration of the $[\text{Eu}(\text{dotagl})]$ at the start of the reaction was 1.0 mM. For the calculation of the first-order rate constants (k_{obs} or k_p), the absorbance values measured at different t times were fit to Eqn. 12, where A_0 , A_t , and A_e are the absorbance values measured at the start of the reaction, at the time t , and at equilibrium, respectively.

$$k_p = \frac{1}{t} \ln \frac{(A_0 - A_e)}{(A_t - A_e)} \quad (12)$$

REFERENCES

- [1] 'The Chemistry of Contrast Agents in Medical Magnetic Resonance Imaging', Eds. A. E. Merbach and É. Tóth, Wiley, New York, 2001.
- [2] P. Caravan, J. J. Ellison, T. J. McMurry, R. B. Lauffer, *Chem. Rev.* **1999**, 99, 2293.
- [3] K. Micskei, L. Helm, E. Brücher, A. E. Merbach, *Inorg. Chem.* **1993**, 32, 3844.
- [4] S. Aime, A. Barge, M. Botta, D. Parker, A. S. DeSousa, *J. Am. Chem. Soc.* **1997**, 119, 4767.

- [5] S. Aime, A. Barge, A. S. Batsanov, M. Botta, D. D. Castelli, F. Fedeli, A. Mortillaro, D. Parker, H. Puschmann, *Chem. Commun.* **2002**, 1120.
- [6] S. Zhang, K. Wu, A. D. Sherry, *J. Am. Chem. Soc.* **2002**, *124*, 4226.
- [7] S. Zhang, P. Winter, K. Wu, A. D. Sherry, *J. Am. Chem. Soc.* **2001**, *123*, 1517.
- [8] S. Zhang, L. Michaudet, S. Burgess, A. D. Sherry, *Angew. Chem., Int. Ed.* **2002**, *41*, 1919.
- [9] S. Aime, D. D. Castelli, E. Terreno, *Angew. Chem., Int. Ed.* **2002**, *41*, 4334.
- [10] S. Aime, A. Barge, D. D. Castelli, F. Fedeli, A. Mortillaro, F. U. Nielsen, E. Terreno, *Magn. Reson. Med.* **2002**, *47*, 639.
- [11] S. Zhang, M. Merrit, D. E. Woessner, R. E. Lenkinski, A. D. Sherry, *Acc. Chem. Res.* **2003**, *36*, 783.
- [12] K. M. Ward, A. H. Aletas, R. S. Balaban, *J. Magn. Reson.* **2000**, *143*, 79.
- [13] D. L. Rabenstein, *Can. J. Chem.* **1972**, *50*, 1036.
- [14] C. F. G. C. Geraldés, A. M. Urbano, M. C. Alpoim, A. D. Sherry, K.-T. Kuan, R. Rajagopalan, F. Maton, R. N. Muller, *Magn. Reson. Imaging* **1995**, *13*, 401.
- [15] H. Imura, G. R. Choppin, W. P. Chacheris, L. A. de Learie, T. J. Dunn, D. H. White, *Inorg. Chim. Acta* **1997**, *258*, 227.
- [16] a) J. F. Desreux, E. Merciny, M. F. Lincoln, *Inorg. Chem.* **1981**, *20*, 987; b) R. Delgado, J. J. Frausto Da Silva, *Talanta* **1982**, *29*, 815.
- [17] S. Zhang, K. Wu, M. C. Biewer, A. D. Sherry, *Inorg. Chem.* **2001**, *40*, 4284.
- [18] D. A. Voss, E. R. Farquhar, W. D. Horrocks Jr., J. R. Morrow, *Inorg. Chim. Acta* **2004**, *357*, 859.
- [19] 'Critical Stability Constants', Vol. 1, Ed. A. E. Martell, Plenum, New York, 1974.
- [20] H. Sigel, R. B. Martin, *Chem. Rev.* **1982**, *82*, 385.
- [21] W. D. Kim, G. E. Kiefer, F. Maton, K. McMillan, R. N. Muller, A. D. Sherry, *Inorg. Chem.* **1995**, *34*, 2233.
- [22] S. Aime, M. Botta, M. Fasano, S. Paoletti, P. L. Anelli, F. Uggeri, M. Virtuani, *Inorg. Chem.* **1994**, *33*, 4707.
- [23] E. Brücher, G. Laurenczy, Z. Makra, *Inorg. Chim. Acta* **1987**, *139*, 141.
- [24] X. Wang, T. Jin, V. Comblin, A. Lopez-Mut, E. Merciny, J. F. Desreux, *Inorg. Chem.* **1992**, *31*, 1095.
- [25] É. Tóth, E. Brücher, I. Lázár, I. Tóth, *Inorg. Chem.* **1994**, *33*, 4070.
- [26] S. L. Wu, W. D. Horrocks Jr., *Inorg. Chem.* **1995**, *34*, 3724.
- [27] K. Kumar, M. F. Tweedle, *Inorg. Chem.* **1993**, *32*, 4193.
- [28] L. Burai, I. Fábrián, R. Király, E. Szilágyi, E. Brücher, *J. Chem. Soc., Dalton Trans.* **1998**, 243.
- [29] H. M. Irving, M. G. Miles, L. Pettit, *Anal. Chim. Acta* **1967**, *28*, 475.
- [30] L. Zékány, I. Nagypál, in 'Computational Methods for Determination of Formation Constants', Ed. D. J. Legett, Plenum, New York, 1985, p. 291.

Received November 22, 2004